

Wake transition of two-dimensional cylinders and axisymmetric bluff bodies

M. C. Thompson*

Abstract

This article presents an overview of the instability modes occurring in wakes of two-dimensional cylinders and (axisymmetric) tori. The instabilities are compared and contrasted, especially with reference to the base case of the circular cylinder wake. The latter has been the subject of intense interest and scrutiny for well over a century, and has implicitly assumed the role of providing the generic transition scenario to turbulent wake flow. In particular, it is observed that for elongated cylinders with streamlined leading edges, the analogues of the instability modes for a circular cylinder become unstable in the reverse order, which may have implications for the route to wake turbulence for such bodies. As well, the analogue of mode B has a significantly increased relative spanwise wavelength and appears to have a different structure in the near wake. At the other extreme, for a normal flat plate, the wake first becomes unstable to a non-periodic mode that appears distinct from either of the dominant circular cylinder wake modes. For tori, which have a local geometry approaching a two-dimensional circular cylinder for high aspect ratios, the first occurring wake instability mode is a subharmonic mode for intermediate aspect ratios.

Possible underlying physical mechanisms leading to some of these instabilities are also examined. In particular, support is provided for the role of idealised physical instability mechanisms in controlling wavelength selection and amplification for the dominant cylinder wake modes. The results presented in this article focus on relevant research undertaken by the Monash group but draws in results from many other international groups.

Introduction

Considerable experimental and computational effort has gone into documenting the three-dimensional wake transitions of a nominally two-dimensional circular cylinder. A non-exhaustive sample of articles include Williamson (1988*b*, 1996*b,a*); Wu *et al.* (1996); Thompson *et al.* (1994, 1996); Barkley & Henderson (1996); Henderson (1997); Mittal & Balachandar (1995); Karniadakis & Trintafyllou (1992); Brede *et al.* (1996); Bays-Muchmore & Ahmed (1993); Gerrard (1978). Stability analysis (Barkley & Henderson (1996)) indicates that the two-dimensional wake becomes linearly unstable to mode A at $Re \simeq 190$, and the base flow undergoes a further bifurcation to mode B at $Re \simeq 260$. Experiments (Williamson (1988*b*); Miller & Williamson (1994)) and DNS (Thompson *et al.* (1996); Henderson (1997)) simulations show that this mode becomes unstable at lower Reynolds number because the saturation of mode A significantly modifies the wake structure. There is a strong interaction between the modes and the wake undergoes a rapid transition to spatio-temporal chaos (Henderson (1997)), so that it is effectively turbulent for a Reynolds number of just a few hundred. The saturation of the modes in the wake have also been modelled in detail using the Landau equation (Henderson (1997)). Finally the physical mechanism driving the instability modes has been explored by various authors including Barkley & Henderson (1996); Henderson (1997); Leweke & Williamson (1998); Thompson *et al.* (2001*b*). Figure 1 shows a side-by-side comparison of experimental and numerical tracer visualisations of the mode A and B shedding modes. So it appears that this wake has been well documented and is well understood; however, an obvious question is whether this transition scenario is generic or universal for a variety of other two-dimensional and axisymmetric body shapes. This question is addressed by the current paper.

The FLAIR (Fluids Laboratory for Aeronautical and Industrial Research) group at Monash University has spent considerable effort investigating the effect of body shape on wake transition. Two broadly representative sequences of body geometry have been examined. The first set consists of the normal flat plate, a circular cylinder, and elongated cylinders with elliptical-leading edges to prevent vortex shedding except from the trailing edge. The second set focusses on axisymmetric bodies, in particular a ring or torus placed with its axis

*Department of Mechanical Engineering, Monash University, Clayton, AUSTRALIA. <mailto:mark.thompson@eng.monash.edu.au>

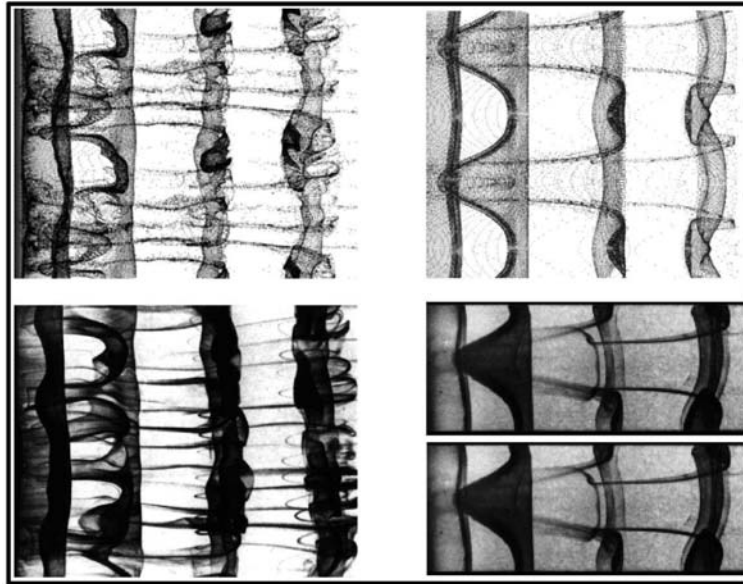


Figure 1: Numerical visualisations of the two shedding modes using passive tracer particles (top) compared with experimental dye visualisations obtained by Charles Williamson. Mode B is shown at the left and mode A at the right.

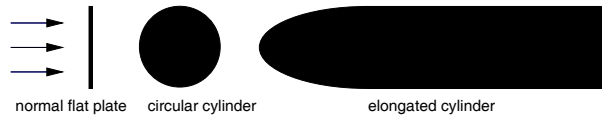
aligned with the flow direction. By adjusting the aspect ratio, it can be transformed continuously from a sphere to a very large ring where curvature effects are negligible, so that a section of the geometry is representative of a circular cylinder. These sequences of body shapes are depicted in figure 2a and b.

Wake transition of two-dimensional bodies

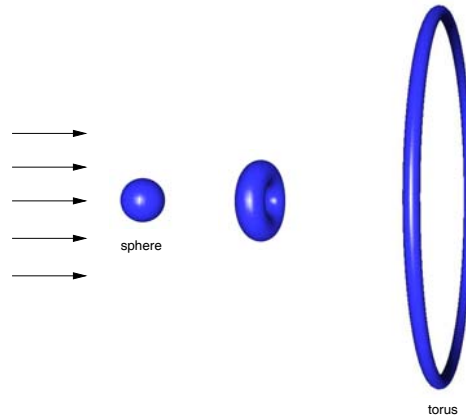
Circular and square cylinders

As mentioned above, the three-dimensional transitions in a wake of a circular cylinder have been extensively studied experimentally, numerically and theoretically. The wake becomes unstable to three-dimensional perturbations through a subcritical (i.e., hysteretic) transition (Henderson (1997)) to an instability mode, dubbed mode A by Williamson (1988a) (also see Williamson (1996b,a)), at $Re \simeq 190$. The wavelength of this mode is approximately $4D$, where D is the cylinder diameter. Experimentally it is found that the saturated mode is not periodic, at least for Reynolds number not too far in excess of transition. DNS simulations at $Re = 210$, have confirmed this behaviour (Sheard, private communication; also see Henderson (1997)). Floquet stability analysis (Barkley & Henderson (1996)) of the two-dimensional base flow indicates that a second mode, known as mode B, becomes unstable at $Re \simeq 260$. This has a much shorter wavelength of $\lambda/D \simeq 0.8$. In experiments and DNS simulations this mode is seen at much lower Reynolds numbers, $Re \gtrsim 230$, presumably due to the modification of the previously two-dimensional wake by the saturated mode A state. The wake becomes chaotic rapidly with increasing Reynolds number through spatio-temporal chaos (Henderson (1997)), and is effectively turbulent at $Re \gtrsim 300$. Importantly, the wake continues to show strong evidence of the mode B wavelength at much higher Reynolds numbers (Wu *et al.* (1996)) and presumably it contributes significantly to lateral mixing.

Robichaux *et al.* (1999) performed a Floquet stability analysis of the wake of a square cylinder. The transition scenario appears to be similar to the circular cylinder. Again, mode A and B occur in the same sequence with transition Reynolds numbers of about 160 and 190, respectively. The maximally amplified wavelengths are also similar at 1.2 and 5.5 times the cylinder height. Interestingly, if the scale length is taken as the length of the diagonal, the preferred wavelengths are the same as for the circular cylinder to within a few percent. These authors also found a further instability mode, which they called mode S (for subharmonic). This occurred at a higher critical Reynolds number of $Re = 200$, and had a wavelength in between the mode A and B wavelengths. Blackburn & Lopez (2003) subsequently showed that, in fact, this mode was not a subharmonic, but was a mode with a complex Floquet multiplier with a period of approximately twice the base flow period. A theoretical analysis based on symmetry groups (Blackburn *et al.* (2005)) of the possible modes for geometries with this set of flow symmetries, indicated the only modes with the time-space symmetries of mode A and B could occur. The occurrence of a true subharmonic mode would be extremely unlikely.



(a)



(b)

Figure 2: Top: Sequence of two-dimensional cylinders used to study two-dimensional wake evolution. Bottom: Axisymmetric bodies examined.



Figure 3: Two-dimensional coloured vorticity contours showing the shedding pattern for flow past a normal flat plate. Flow is from left to right. Left to right: $Re = 40, 80$ and 130 , respectively.

Normal flat plate

As for the circular cylinder there is only a single separation point on each side of the wake, although it is fixed in position. At low Reynolds numbers the wake resembles the typical Karman wake of a circular cylinder. As the Reynolds number is increased the wake rapidly evolves spatially downstream to two sets of positive and negative vortices distributed on either side of the wake centerline. The two-dimensional wake as depicted by coloured vorticity contours is shown in figure 3 for Reynolds numbers of 40, 80 and 130. Relevant previous research includes Najjar & Balachandar (1997), who performed a three-dimensional numerical study of the three-dimensional wake at $Re = 250$, and Julien *et al.* (2004, 2003) who examined the stability modes for an idealised wake based on the wake from a normal flat plate.

Figure 4 shows dominant Floquet multipliers against wavelength for a number of Reynolds numbers. There are two dominant modes, the longer wavelength mode is the first to go unstable at $Re \simeq 115$, and has a preferred wavelength of approximately $5-6H$, where H is the height of the plate. In this case, the dominant mode has a complex multiplier (indicated by the dashed line). The shorter wavelength mode has a dominant wavelength of $\lambda/H \simeq 2$ becoming unstable at $Re \simeq 125$.

Given the quite different structure of the vortex street, it is perhaps not surprising that the mode shapes are quite different from those of a circular cylinder. Figure 5 shows perturbation spanwise vorticity contours for the shorter and longer wavelength modes. The position of the spanwise vortex structures are indicated as well. The shorter mode has the same spatio-temporal symmetry as mode A of the circular cylinder. In addition, there is strong evidence of elliptical instability in the vortex cores, consistent with mode A. The longer

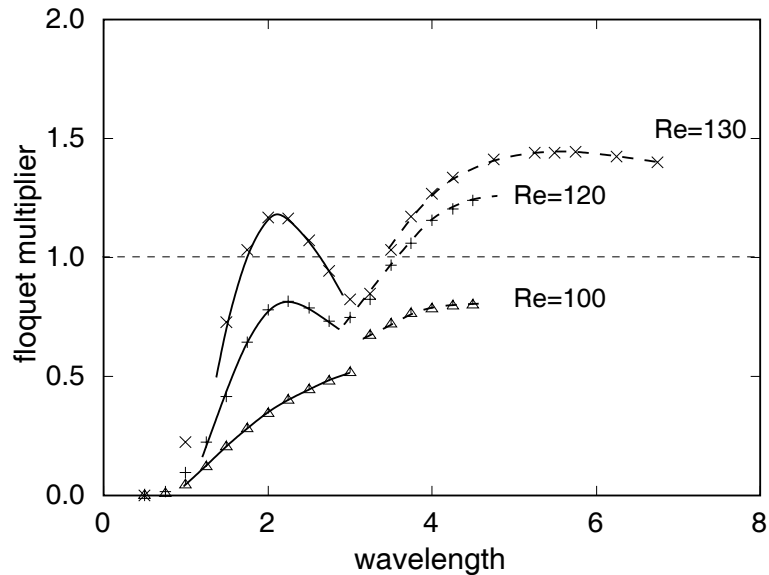


Figure 4: Dominant Floquet multipliers for the wake of a normal flat plate.

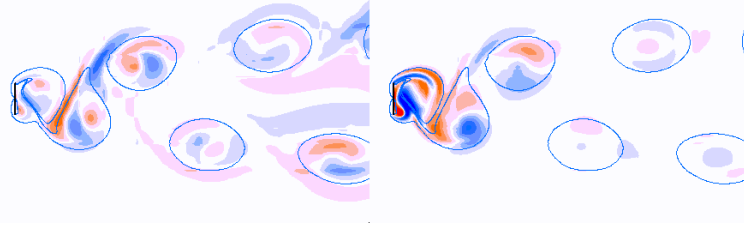


Figure 5: Spanwise perturbation vorticity structure of the first two instability modes for the normal flat plate. The left and right images corresponds to a wavelengths of $\lambda/H = 2$ and 5.5 , respectively. The Reynolds number is 130.

spanwise wavelength mode is strong close to the rear of the plate but decays rapidly with downstream distance. As mentioned, the Floquet multiplier is complex before and after transition, and the period of the mode is not commensurate with the base flow period. Indeed, the period is highly variable with wavelength, which may indicate the rapid development of a very chaotic wake with increasing Reynolds number.

Elongated cylinders

Results for this body geometry have been presented in Ryan *et al.* (2005). A summary of the key findings are presented here.

In this case there are three unstable modes denoted mode A, B' and S', in line with the modes observed for square and circular cylinders. The critical wavelengths of these modes are approximately 4, 2.2 and 1 cylinder widths. Mode A is topologically similar to mode A for a circular cylinder as can be seen by a comparison of perturbation spanwise vorticity contours in figure 7. Mode B' has the same spatio-temporal symmetry as mode B of a circular cylinder; however, there are some other significant differences (hence the dash). The preferred wavelength is considerably longer (2.2 compared with 0.82) and the perturbation field in the near wake is markedly different. Nonetheless, the downstream development is very similar. Mode S' is in some senses similar to the *almost* subharmonic mode observed by Robichaux *et al.* (1999). Again, the mode has a complex Floquet multiplier, although it is not close to having a subharmonic period. The real part of the Floquet multiplier only becomes greater than unity for large aspect ratio cylinders. Isosurface visualisations depicting streamwise vorticity are given in figure 6.

Figure 8 shows the variation of critical Reynolds number as a function of aspect ratio for modes A and B'. The most striking feature is that mode B' becomes unstable at a lower Reynolds number for cylinders with length to height ratios greater than approximately 7. Indeed for a cylinder with length to height ratio is 17.5, the difference in the critical Reynolds numbers is close to 300. Given that Karniadakis & Trintafyllou (1992)

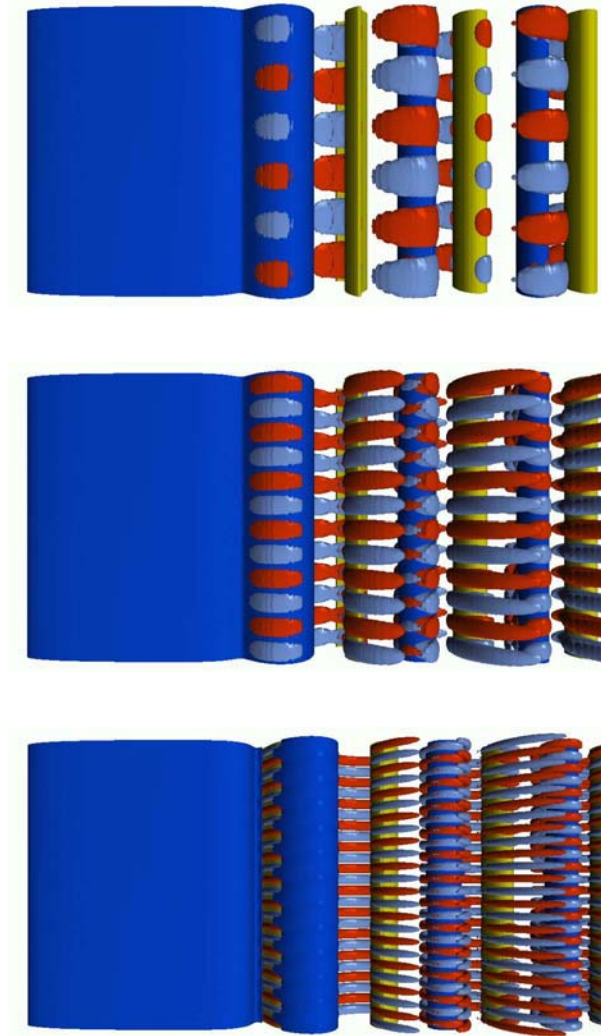


Figure 6: Isosurfaces of the streamwise vorticity field for the three identified instability modes (A, B' & S') for an elliptical leading-edge cylinder. Isosurfaces of spanwise vorticity show the positions of the Karman vortices. The span length is $12H$.

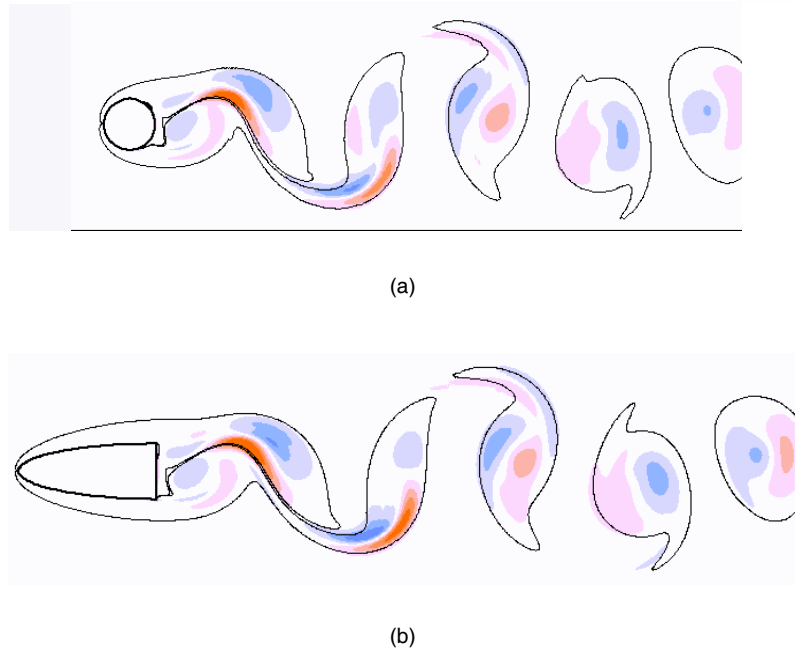


Figure 7: Comparison of the wake spanwise vorticity field of the Floquet mode for a circular cylinder ($Re = 190, \lambda = 4D$) and short plate ($AR = 2.5, Re = 240, \lambda = 4H$) showing the longer wavelength instability for the short plate is analogous to the Mode A instability of the circular cylinder. The spatial structure of the perturbation field relative to the position of the Karman vortices is highlighted by the contours of spanwise vorticity with $\omega_z = \pm 0.2$. Both images are at approximately the same phase in the shedding cycle.

found that mode B underwent period-doubling when the existence of mode A was suppressed by artificially restricting the spanwise domain, it is not clear that the transition to turbulence will occur through the same route for elongated cylinders as for short cylinders.

Wake transition of axisymmetric bodies

Sphere

This case has been studied extensively by many research groups over the years. The wake transitions are quite distinct from those for a circular cylinder wake. The wake undergoes a regular (i.e., time-steady) transition at $Re = 212$ to the beautiful two-threaded wake (Margarvey & Bishop (1961a,b); Johnson & Patel (1999); Tomboulides *et al.* (1993, 2000); Thompson *et al.* (2001a); Ghidsera & Dusek (2000); Ormières & Provansal (1999)). This wake then becomes unstable at ($Re = 270$) through a Hopf (steady to periodic) bifurcation. At $Re \simeq 350$ the orientation of the shed vortical structures loses coherence (Mittal (1999)). The overall wake structure is similar at considerably higher Reynolds numbers, although much more chaotic.

Tori

Sheard has undertaken an extensive numerical study of aspects of flows past spheres, including three-dimensional transitions (Sheard *et al.* (2003)), DNS simulations and Landau modelling examining the saturation of the instability modes (Sheard *et al.* (2004)), and examining wake transition to a subharmonic mode for a torus of a specific aspect ratio (Sheard *et al.* (2005)).

As the aspect ratio (ring diameter to cylinder cross-section diameter) becomes large so that curvature effects become small, then locally the body geometry approaches the geometry of a two-dimensional circular cylinder. Indeed, this was part of the motivation for the experimental study of Leweke & Provansal (1995). The other motivating factor was the elimination of end effects, which complicate the experimental study of circular cylinder wakes. For large aspect ratios the analogues of modes A and B also occur for this geometry, with similar preferred wavelengths. Even for large aspect ratio tori, the ring curvature leads to a loss of the symmetry in the plane defined by the flow direction and cylinder axis for a two-dimensional cylinder. This change to symmetry group properties allows a true subharmonic mode to develop (mode C), which is in

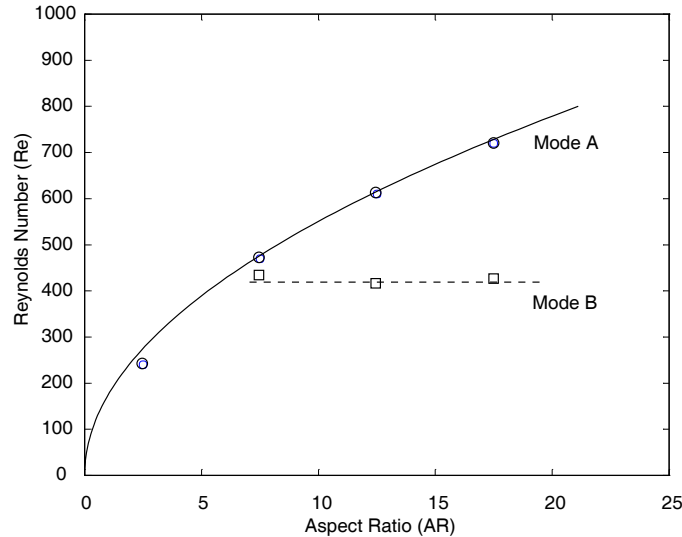


Figure 8: Critical Reynolds number for the different mode transitions as a function of plate aspect ratio. Here, \square indicates a Mode B' transition and \circ indicates a Mode A transition. The curves represent an approximate fit to the data.

fact the first occurring instability mode for tori of aspect ratios $4 \lesssim Ar \lesssim 8$. DNS simulations supported by experimental visualisations have confirmed the occurrence of this mode shown in figure 9.

Physical mechanisms of transition

There has been debate over the physical mechanisms responsible for the development of these instabilities. There have been suggestions that mode A is due to a Benjamin-Feir instability (Leweke & Provansal (1995)), a centrifugal instability of the braid region between the main vortex rollers (Brede *et al.* (1996)), and an elliptical instability of the vortex cores (Leweke & Williamson (1998); Thompson *et al.* (2001b)). Speculation has also occurred for mode B, certainly in terms of a three-dimensional shear layer instability of the separating shear layers (Brede *et al.* (1996)), a centrifugal instability (Ryan *et al.* (2005)) and a hyperbolic instability of the braid region (Leweke & Williamson (1998)). Naturally, the flow field is complex and hence it is not clear that the development of an instability can be entirely attributed to a unique physical instability mechanism that governs a very simple flow topology. Nevertheless, it is appealing to do this to provide some physical insight into the evolution of the flow as the Reynolds number is increased.

For mode A, it appears elliptical instability strongly contributes to the development of the instability. Williamson (1996b,a) suggested that for a circular cylinder mode, the instability modes scale with the wake vortex cores (mode A) and the width of the braids between the cores (mode B). Leweke & Williamson (1998) explored the possibility that mode A was primarily elliptic in origin by analytically calculating the growth rate of the strained vortex cores to an elliptic instability. The growth over a cycle was found to be substantial and it was speculated that this would provide sufficient feedback from one shedding cycle to the next to sustain the instability. In addition, the analytically-predicted spanwise wavelength for elliptic instability closely matched the experimentally-observed and numerically-predicted wavelength. Thompson *et al.* (2001b) examined the growth of the mode through DNS simulations. These showed that as each pair of wake vortices form and begin to shed, the perturbation fields within the cores are locally consistent with the signature of elliptic instability. Effectively, a cooperative elliptic instability (Leweke & Williamson (1998)) develops between the shedding vortices. However, the perturbation then grows rapidly between the cores, where the flow is undergoing rapid straining. DNS simulations established that the mode A field would recover more quickly if the perturbation field was artificially zeroed in the parts of the domain where the flow was hyperbolic rather than elliptic. It appears that the instability is slaved to the elliptic core instability. Julien *et al.* (2004) found similar behaviour occurring between vortex cores for Bickley flow as an idealised model of the wake from a normal flat plate. Again, the core instability controls the wavelength and overall growth rate although the perturbation field appears strong between the cores.

Mode B shows strong growth in the braids and between the forming Karman vortices. The development of the perturbation field within the vortex cores is much reduced and does not show the signature of an elliptic instability. Indeed, the preferred wavelength is probably too small for amplification through an elliptic mecha-

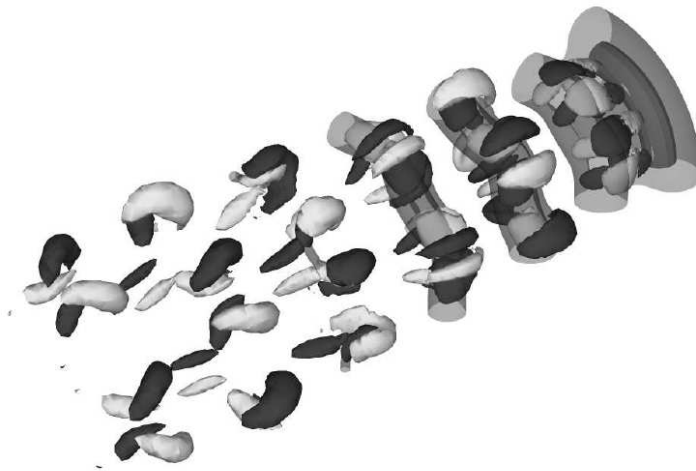


Figure 9: Perspective view of mode C shedding from a torus of aspect ratio 5 at $Re = 190$, from DNS. The flow is from the top right to bottom left. Only a section of the torus is shown to more clearly show the subharmonic nature of the mode. Greyscale streamwise perturbation isosurfaces are used to visualise the mode.

nism. In Ryan *et al.* (2005) an attempt is made to associate the instability with a centrifugal instability. The spatio-temporal topology of the mode is consistent with a centrifugal instability, in that the streamwise vortices identified with the development of the perturbation extend downstream as unbroken tubes along the braids. This provides a feedback mechanism from one cycle to the next, sustaining the perturbation. A idealised stability analysis based on isolating part of the near wake region where the growth rate is large, shows that the predicted instability wavelength is within 25% of the preferred wavelength of mode B. In addition, the predicted growth rate applicable to the time taken for fluid parcels to travel through this region on circular streamlines is also within 30% of the total growth measured directly from DNS for the corresponding time.

References

- BARKLEY, D. & HENDERSON, R. 1996 Three-dimensional floquet stability analysis of the wake of a circular cylinder. *J. Fluid Mech.* **322**, 215–241.
- BAYS-MUCHMORE, B. & AHMED, A. 1993 On streamwise vortices in turbulent wakes of a cylinder. *Phys. Fluids A* **5**(2), 387.
- BLACKBURN, H. M. & LOPEZ, J. M. 2003 On three-dimensional quasiperiodic floquet instabilities of two-dimensional bluff body wakes. *Phys. Fluids* **15**, L57–L60.
- BLACKBURN, H. M., MARQUES, F. & LOPEZ, J. M. 2005 Symmetry breaking of two-dimensional time-periodic wakes. *J. Fluid Mech.* **552**, 395–411.
- BREDE, M., ECKELMANN, H. & ROCKWELL, D. 1996 On secondary vortices in a cylinder wake. *Phys. Fluids* **8**, 2117–2124.
- GERRARD, J. H. 1978 The wakes of cylindrical bluff bodies at low reynolds numbers. *Philos. Trans. R. Soc. London Ser. A* **288**, 351–382.
- GHIDSERA, B. & DUSEK, J. 2000 Breaking of axisymmetry and onset of unsteadiness in the wake of a sphere. *J. Fluid Mech.* **423**, 33–69.
- HENDERSON, R. 1997 Nonlinear dynamics and pattern formation in turbulent wake transition. *J. Fluid Mech.* **352**, 65–112.
- JOHNSON, T. & PATEL, V. 1999 Flow past a sphere up to a reynolds number of 300. *J. Fluid Mech.* **378**, 19–70.
- JULIEN, S., LASHERAS, J. & CHOMAZ, J. 2003 Three-dimensional instability and vorticity patterns in the wake of a flat plate. *J. Fluid Mech.* **479**, 155–189.

- JULIEN, S., ORTIZ, S. & CHOMAZ, J.-M. 2004 Secondary instability mechanisms in the wake of a flat plate. *European Journal of Mechanics B/Fluids* **23** (1), 157–165.
- KARNIADAKIS, G. E. & TRINTAFYLLOU, G. S. 1992 Three-dimensional dynamics and transition to turbulence in the wake of bluff objects. *J. Fluid Mech.* **238**, 1–30.
- LEWEKE, T. & PROVANSAL, M. 1995 The flow behind rings: Bluff body wakes without end effects. *J. Fluid Mech.* **288**, 265–310.
- LEWEKE, T. & WILLIAMSON, C. H. K. 1998 Cooperative elliptic instability of a vortex pair. *J. Fluid Mech.* **360**, 85–119.
- LEWEKE, T. & WILLIAMSON, C. H. K. 1998 Three-dimensional instabilities in wake transition. *European Journal of Mechanics B/Fluids* **17**, 571–586.
- MARGARVEY, R. & BISHOP, R. 1961a Transition ranges for three-dimensional wakes. *Canadian J. Phys.* **39**, 1418–1422.
- MARGARVEY, R. & BISHOP, R. 1961b Wakes in liquid-liquid systems. *Phys. Fluids* **4** (7), 800–805.
- MILLER, G. D. & WILLIAMSON, C. H. K. 1994 Control of three-dimensional phase dynamic in a cylinder wake. *Experiments in Fluids* **18**, 26.
- MITTAL, R. 1999 Planar symmetry in the unsteady wake of a sphere. *AIAA J.* **37** (3), TN 388–390.
- MITTAL, R. & BALACHANDAR, S. 1995 Generation of streamwise structures in bluff body wakes. *Phys. Rev. Lett.* **75**, 1300.
- NAJJAR, F. M. & BALACHANDAR, S. 1997 Low-frequency unsteadiness in the wake of a normal flat plate. *J. Fluid Mech.* **370**, 101–147.
- ORMIÈRES, D. & PROVANSAL, M. 1999 Transition to turbulence in the wake of a sphere. *Phys. Rev. Lett.* **83**, 80–83.
- ROBICHAUX, J., BALACHANDAR, S. & VANKA, S. P. 1999 Three-dimensional floquet instability of the wake of square cylinder. *Phys. Fluids* **11**, 560–578.
- RYAN, K., THOMPSON, M. C. & HOURIGAN, K. 2005 Three-dimensional transition in the wake of elongated bluff bodies. *J. Fluid Mech.* **in press**.
- SHEARD, G., THOMPSON, M. & HOURIGAN, K. 2003 From spheres to circular cylinders: the stability and flow structures of bluff ring wakes. *J. Fluid Mech.* **492**, 147–180.
- SHEARD, G., THOMPSON, M. & HOURIGAN, K. 2004 From spheres to circular cylinders: Non-axisymmetric transition in the flow past rings. *J. Fluid Mech.* **506**, 45–78.
- SHEARD, G., THOMPSON, M., HOURIGAN, K. & LEWEKE, T. 2005 The evolution of a subharmonic mode in a vortex street. *J. Fluid Mech.* **in press**.
- THOMPSON, M., HOURIGAN, K. & SHERIDAN, J. 1994 Three-dimensional instabilities in the cylinder wake. In *Int. Colloq. Jets, Wakes, Shear Layers*. Melbourne, Aust.
- THOMPSON, M., LEWEKE, T. & PROVANSAL, M. 2001a Kinematics and dynamics of sphere wake transition. *J. Fluids Struct.* **15**, 575–585.
- THOMPSON, M., LEWEKE, T. & WILLIAMSON, C. 2001b The physical mechanism of transition in bluff body wakes. *J. Fluids Struct.* **15**, 607–616.
- THOMPSON, M. C., HOURIGAN, K. & SHERIDAN, J. 1996 Three-dimensional instabilities in the wake of a circular cylinder. *Experimental Thermal and Fluid Science* **12**, 190–196.
- TOMBOULIDES, A., ORZSAG, S. & KARNIADAKIS, G. 1993 Direct and large eddy simulations of axisymmetric wakes. *AIAA paper* **93-0546**.
- TOMBOULIDES, A., ORZSAG, S. & KARNIADAKIS, G. 2000 Numerical investigation of transitional and weak turbulent flow past a sphere. *J. Fluid Mech.* **416**, 45–73.

- WILLIAMSON, C. H. K. 1988a Defining a universal and continuous strouhal-reynolds number relationship for the laminar vortex shedding of a circular cylinder. *Phys. Fluids* **31**, 2742–2744.
- WILLIAMSON, C. H. K. 1988b The existence of two stages in the transition to three dimensionality of a cylinder wake. *Phys. Fluids* **31**, 3165–3168.
- WILLIAMSON, C. H. K. 1996a Three-dimensional wake transition. *J. Fluid Mech.* **328**, 345–407.
- WILLIAMSON, C. H. K. 1996b Vortex dynamics in the cylinder wake. *Annual Review of Fluid Mechanics* **28**, 477–539.
- WU, J., SHERIDAN, J., WELSH, M. C. & HOURIGAN, K. 1996 Three-dimensional vortex structures in a cylinder wake. *J. Fluid Mech.* **312**, 201–222.